G-Tech : Jurnal Teknologi Terapan
Vol. 10, No. 1, January 2026, p. 398-408
E-ISSN: 2623-064X | P-ISSN: 2580-8737

YOLO-Based Pedestrian Trajectory Analysis for Zebra Crossing Safety and Suitability Evaluation Using UAV Data

Arde Dewantara Herjuna[1]✉, Anak Agung Gde Kartika[2], Pujo Aji[3]

[1, 2, 3] Department of Civil Engineering, Faculty of Civil, Planning and Geo Engineering, Institutt Teknologi Sepuluh Nopember, Indonesia

✉ **Corresponding Author :** Arde Dewantara Herjuna (e-mail: ardewantara@gmail.com)

Article Information

Article History

Received : December 14, 2025
Revised : January 10, 2026
Published : January 16, 2026

***Keywords*:**

Deep Learning;
Drone;
Pedestrian Trajectory;
YOLO.

ABSTRACT

Pedestrian crossing facilities in urban areas are often positioned without adequate consideration of actual movement patterns, leading to low utilization rates, widespread informal crossings, and increased pedestrian-vehicle conflict risks. Traditional manual observation methods for assessing crossing behavior are time-consuming, subjective, and unable to capture continuous spatial-temporal movement dynamics at scale. This study aims to develop and evaluate an automated framework for extracting pedestrian trajectories and assessing the alignment between pedestrian desire lines and existing zebra crossing infrastructure. The methodology integrates YOLO11 fine-tuned object detection with ByteTrack multi-object tracking to process unmanned aerial vehicle (UAV) video data collected at an urban intersection in Surabaya, Indonesia. Pedestrian-vehicle conflict severity was quantified using Time-to-Collision (TTC)-based surrogate safety indicators, including Time Exposed to Time-to-Collision (TET) and Time Integrated Time-to-Collision (TIT). The results reveal substantial heterogeneity in crossing behavior, with distinct spatial clustering of informal crossing hotspots located away from the designated zebra crossing. Asymmetric yet bidirectional pedestrian demand patterns were observed across the study area. Based on trajectory-derived evidence, the study recommends strategic relocation of the zebra crossing approximately 135 meters south to better accommodate natural pedestrian flow and reduce vehicular traffic exposure. These findings demonstrate that deep learning-based trajectory analysis offers a practical, objective, and scalable approach for evidence-based pedestrian infrastructure planning, particularly applicable to rapidly urbanizing contexts in developing countries where conventional assessment resources are limited.

INTRODUCTION

Pedestrian mobility constitutes a fundamental component of urban transport systems and is closely associated with safety, accessibility, and sustainability objectives. In urban environments, marked pedestrian crossings such as zebra crossings are commonly implemented to facilitate safe road crossing. However, the presence of designated crossing facilities does not necessarily ensure their use. Empirical observations indicate that pedestrians frequently deviate from designated crossings and instead utilize informal paths that better align with their origin-destination trajectories. Such deviations may reduce compliance and increase exposure to vehicle-pedestrian conflicts, thereby raising safety concerns (Retnowati et al., 2022).

This is an open access article under the CC BY license

Similar patterns have been reported in other developing-country contexts, where pedestrians frequently avoid designated crossings and instead choose informal crossing points that minimize walking distance or better match their travel needs (Ardiansah et al., 2020; Khalak et al., 2024). Studies at signalized and unsignalized zebra crossings further demonstrate that utilization rates are strongly influenced by spatial relevance, crossing distance, and surrounding traffic conditions (Al Bargi et al., 2023; Ismail et al., 2023). These findings suggest that informal crossing behavior is not merely a compliance issue, but rather a structural consequence of crossing facilities that are insufficiently aligned with pedestrian desire lines.

Conventional methods for analyzing pedestrian crossing behavior rely primarily on manual observation and field surveys. While these approaches provide valuable descriptive insights, they are limited in their ability to capture continuous pedestrian trajectories and fine-grained spatial-temporal interactions. Recent advances in computer vision and deep learning enable automated detection and tracking of pedestrians from aerial video data, offering new opportunities for large-scale and objective behavioral analysis (Braun et al., 2018; Fourkiotis et al., 2022; Li et al., 2024). Drone-based datasets have been successfully used to extract naturalistic road-user trajectories, although their primary application has focused on automated driving research rather than pedestrian infrastructure evaluation (Bock et al., 2019). Similarly, studies employing deep learning for pedestrian-related infrastructure analysis have largely emphasized asset detection and condition assessment, rather than linking observed pedestrian movement patterns to the performance or suitability of crossing facilities (Antwi et al., 2025; Rosa et al., 2024). Recent surveys on deep learning-based pedestrian trajectory prediction identify motion uncertainty, interaction modeling, and scene context understanding as persistent challenges, while approaches incorporating recurrent architectures and attention mechanisms demonstrate strong potential for capturing complex pedestrian movement patterns in urban environments (Jiang et al., 2025)

Based on these gaps, this study develops and evaluates an automated framework in which YOLO functions as the core pedestrian detection module for extracting high-resolution spatio-temporal information from UAV video data. YOLO enables reliable frame-level pedestrian identification under real-world traffic conditions, providing a robust foundation for multi-object tracking and continuous trajectory reconstruction. The extracted trajectories are subsequently used to evaluate the spatial alignment between pedestrian desire lines and existing zebra crossing facilities, identify informal crossing hotspots, and quantify pedestrian-vehicle interaction risk using cumulative safety indicators, including Time Exposed to Time-to-Collision (TET), Time Integrated Time-to-Collision (TIT), and braking-based measures. By employing YOLO-driven detection as the primary data acquisition mechanism, this framework supports objective and scalable, evidence-based decisions regarding the placement or relocation of pedestrian crossing facilities in urban environments of developing countries.

RESEARCH METHODS

Research Design

This study adopts a quantitative observational approach to extract and analyze pedestrian movement trajectories using automated video processing based on YOLO-driven detection and ByteTrack-based multi-object tracking. The methodological framework consists of three primary components, namely data acquisition through UAV-based video observation, automated pedestrian trajectory extraction, and the evaluation of pedestrian crossing behavior in relation to existing crossing infrastructure. The study site was selected based on the convergence of multiple high-volume pedestrian generators, including a public school, the city square, and a museum, which produce sustained and diverse pedestrian flow patterns, representing realistic urban infrastructure challenges critical for quantifying conflict severity and operational safety.

Data Collection

Video data were collected using a DJI Mini 3 unmanned aerial vehicle (UAV) positioned directly above the study location on intersection Jalan Gubernur Suryo, Surabaya, Indonesia, producing a nadir viewpoint that minimizes perspective distortion and visual obstruction. All

recordings were captured in 4K resolution at 30 frames per second, with approximately fifteen minutes of continuous footage during peak hour on weekend. The use of UAV-based observation enables unobtrusive monitoring of pedestrian behavior without disrupting naturally occurring movement patterns, which is essential for capturing realistic pedestrian-vehicle interactions (Bock et al., 2019; Parra-Ovalle et al., 2023). Previous studies have demonstrated that UAV data acquisition allows the extraction of large-scale pedestrian trajectories under real-world conditions at relatively low cost and without environmental intervention (Ahmed et al., 2025). Moreover, the integration of UAV imagery with artificial intelligence facilitates the identification of pedestrian-vehicle interactions under dense traffic conditions and enables micro-scale risk mapping, thereby reinforcing the robustness of drone-based data acquisition for trajectory analysis and pedestrian infrastructure performance evaluation (Sun & Pei, 2025).

The nadir-view footage facilitates reliable pedestrian detection and tracking by reducing occlusion and scale variation, thereby improving the performance of convolutional neural network-based detectors such as YOLO(Redmon & Farhadi, 2018). When combined with multi-object tracking algorithms, UAV imagery enables the reconstruction of continuous pedestrian trajectories and the identification of interaction patterns in dense traffic environments(Zhang et al., 2022). Figure 1 illustrates a representative video frame captured from the UAV's nadir perspective, highlighting the spatial coverage and visual clarity used for subsequent pedestrian detection and trajectory extraction.

Figure 1. Point of View Drone

Data Analysis

Figure 2 illustrates the pre-processing workflow applied prior to model training. Raw drone video recordings were first decomposed into individual image frames. Each frame was subsequently partitioned into a 2×2 tiling grid to reduce computational load while preserving spatial resolution for the detection of small objects. Image tiling has been shown to improve detection performance on high-resolution imagery, particularly in visually dense scenes, by enhancing small-object recognition and alleviating memory constraints during large-scale image processing (Ünel et al., 2019).

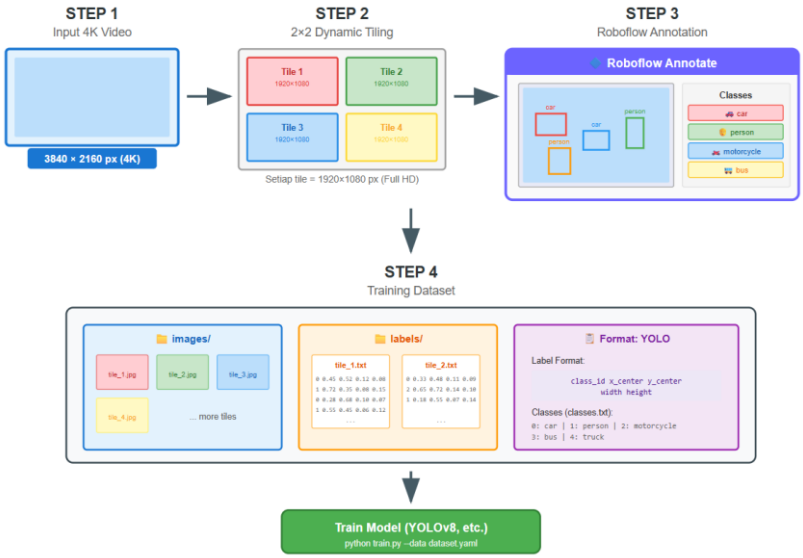

Figure 2. Pre-Processing Workflow

Each image tile was manually annotated using the Roboflow platform to ensure precise bounding box localization. The resulting annotations were converted into the YOLO format and subsequently partitioned into 70 training, 20 validation, and 10 testing subsets. Dataset splitting was conducted using stratified sampling to reduce bias associated with variations in pedestrian density. This approach preserves diversity in density levels across all subsets, thereby supporting robust model evaluation and generalization under varying environmental conditions.

A fine-tuned YOLO11 model was employed as the primary pedestrian detector due to its demonstrated effectiveness in real-time detection under complex outdoor conditions (Qin et al., 2025). Model training was performed for a maximum of 100 epochs using an early stopping strategy with a patience of 20 epochs to mitigate overfitting. Stochastic Gradient Descent was selected as the optimization algorithm, while standard data augmentation techniques were applied to preserve variability in illumination and movement patterns representative of real-world environments. As illustrated in Figure 3, with 1119 dataset the training process converged prior to the maximum epoch limit and was terminated at epoch 75 following the absence of further meaningful performance improvements. The results demonstrate stable convergence, with Precision consistently above 0.85, Recall approaching 0.88, mAP@0.5 reaching approximately 0.89, and mAP@0.5:0.95 stabilizing around 0.72, indicating strong detection accuracy and robustness under varying localization strictness

Figure 3. Training Curves

Figure 4 shows the zoning framework used to ensure that all trajectories, conflict points, and crossing classifications can be spatially interpreted. This zoning is an analytical element enabling evaluation of whether an event constitutes crossing at designated facilities, along desire lines, or as a risky interaction within the roadway area.

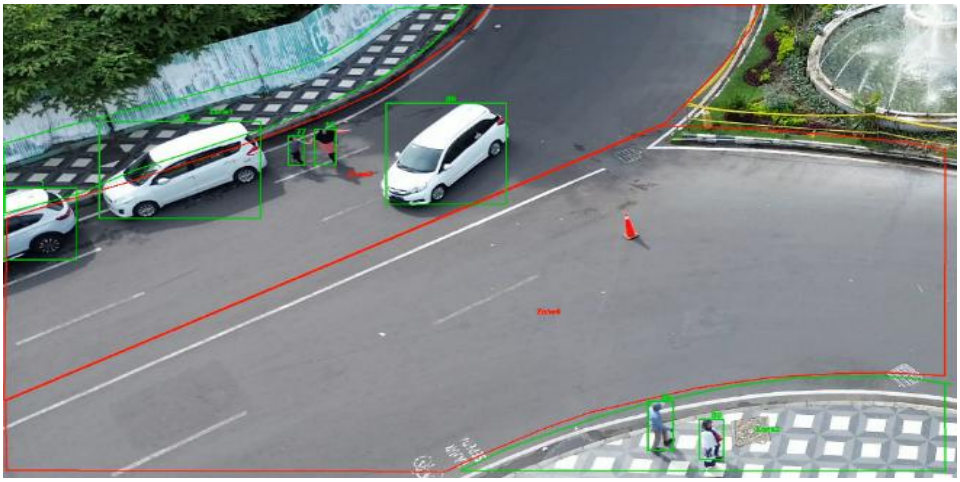

Figure 4. Zoning Framework

The reconstructed trajectories are subsequently analyzed to identify spatial movement patterns, including dominant pedestrian routes and informal crossing locations. These spatial mappings provide the basis for evaluating whether observed crossing behavior aligns with existing infrastructure design or indicates a need for relocation or adaptation of pedestrian crossing facilities.

Vehicle speed estimation is derived from trajectory sequences using frame-to-frame spatio-temporal differences, as expressed in (1). where $\Delta t = 1/\text{FPS}$ represents the time interval between consecutive frames.

$$v(i) = \left(v_x(i), v_y(i)\right) = \frac{1}{\Delta t}(x_i - x_{i-1}, y_i - y_{i-1}) \quad (1)$$

The corresponding scalar speed is computed from the velocity vector using the Euclidean norm, as shown in (2), resulting in continuous speed profiles over time.

$$s(i) = |\mathbf{v}(i)| = \sqrt{v_x(i)^2 + v_y(i)^2} \quad (2)$$

In this formulation, $v_x$and v_y denote the velocity components along the horizontal and vertical axes, respectively, and $\| \mathbf{v} \|$ represents the resulting speed magnitude (Singh et al., 2024). It should be noted that all motion-related measurements are reported in pixel-based units (px and px/s), representing relative displacement in image space rather than absolute physical distance. This approach is commonly adopted in video-based traffic analysis studies where the primary objective is comparative behavioral assessment rather than absolute distance quantification, and where camera calibration data may not be available.

Braking behavior is subsequently analyzed using a 30-frame retrospective window, corresponding to approximately one second at a frame rate of 30 frames per second. This window length is selected to capture short-term speed variations relevant to driver response behavior. Initial and final vehicle velocities are determined as defined in (3) and (4), while deceleration is calculated according to (5).

$$v_{\text{initial}} = \sqrt{\left(\frac{\Delta x}{\Delta t}\right)^2 + \left(\frac{\Delta y}{\Delta t}\right)^2}\Big|_{t=t_0} \quad (3)$$

$$v_{\text{final}} = \sqrt{\left(\frac{\Delta x}{\Delta t}\right)^2 + \left(\frac{\Delta y}{\Delta t}\right)^2}\Big|_{t=t_c} \quad (4)$$

$$a = \frac{v_{\text{final}} - v_{\text{initial}}}{t_{\text{brake}}} \quad (5)$$

In these equations, $v_{\text{init}}$and v_{final} denote the initial and final vehicle speeds within the braking interval, respectively, a represents the longitudinal deceleration rate, and Δt corresponds to the duration of the braking event.

Time-to-Collision is computed as expressed in (6), representing the remaining time until a collision would occur under the assumption that both road users maintain their current velocities and trajectories. In this equation, d denotes the instantaneous separation distance between the pedestrian and the vehicle, and v_{rel} represents the relative approaching speed.

$$\text{TTC} = \frac{d}{v_{\text{rel}}} \tag{6}$$

Time Exposed to Time-to-Collision is calculated as defined in (7). In this formulation, TETrepresents the cumulative duration during which the Time-to-Collision value remains below a predefined critical threshold TTC_{crit}, while Δtdenotes the discrete time interval between successive observations.

$$\text{TET} = \frac{N_{\text{frames}}}{\text{FPS}} \tag{7}$$

Time Integrated Time-to-Collision is computed as expressed in (8) to quantify the cumulative severity of conflict exposure. In this equation, TITrepresents the time-integrated magnitude by which Time-to-Collision falls below the critical threshold TTC_{crit}, and Δt corresponds to the sampling interval between consecutive frames.

$$\text{TIT} = \sum_{i \in F} \frac{\max(0, \tau - \text{TTC}_i)}{\text{FPS}} \tag{8}$$

RESULTS AND DISCUSSION

Pedestrian Trajectory Extraction

The extracted trajectories reveal heterogeneous pedestrian movement patterns under dynamic and variable traffic conditions. Figure 5 presents the trajectory visualization, in which colored paths represent individual pedestrian movements recorded during the observation period. The trajectories capture variations in walking behavior, including speed modulation in response to surrounding traffic, route adjustments associated with informal crossing decisions, and directional changes when interacting with approaching vehicles.

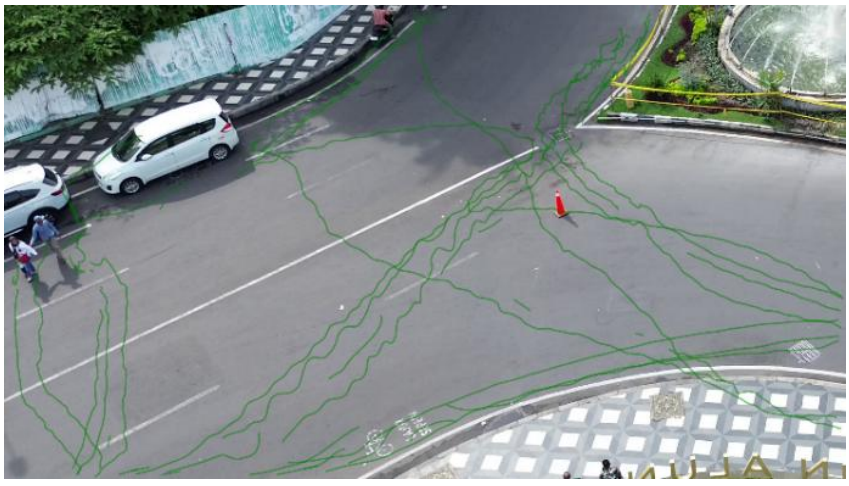

Figure 5. Trajectory Visualization

The spatial density and overlap of trajectories illustrated in Figure 5 highlight key movement characteristics, including dominant pedestrian routes, recurrent decision points where directional changes occur, and high-interaction zones characterized by frequent trajectory

intersections. These spatial patterns provide insight into pedestrian navigation behavior and form the basis for subsequent analyses of crossing behavior and conflict risk.

Based on this quantified evidence, the study proposes a strategic relocation of the zebra crossing facility to better align with observed pedestrian desire lines. As illustrated in Figure 6, the proposed zebra crossing is repositioned at a prominent informal crossing hotspot located approximately 135 meters south of the existing facility. This relocation is intended to reduce unnecessary pedestrian detours and to enhance safety by aligning formal crossing infrastructure with natural movement patterns rather than relying on compliance enforcement.

Figure 6. Proposed Relocation Zebra Cross

The relocation strategy is guided by three primary objectives, namely improving the visibility and accessibility of the crossing facility, reducing pedestrian exposure time to vehicular traffic by shortening effective crossing distances, and providing a more protected crossing environment for high-volume pedestrian corridors. Such design-behavior alignment is critical, as pedestrians are more likely to use formal crossing facilities when these facilities correspond to their natural routes of movement. The necessity for this relocation supports the spatial relevance theory highlighted by Al Bargi et al. (2023) and Ismail et al. (2023), which posits that utilization rates of crossing facilities drop significantly when located beyond a critical tolerance distance from the direct origin-destination path. By shifting the facility 135 meters to match the observed demand peak, the proposed design addresses the structural root cause of non-compliance, rather than attributing it solely to user behavior.

The proposed intervention addresses a structural limitation commonly observed in pedestrian infrastructure planning in Southeast Asia and other developing regions, where conventional planning approaches often overlook empirically derived pedestrian desire lines. By leveraging trajectory-based behavioral evidence, this study offers an objective and data-driven basis for pedestrian facility relocation, supporting infrastructure design decisions grounded in observed behavior rather than prescriptive planning assumptions.

Pedestrian-Vehicle Conflict

Figure 7 presents a representative pedestrian-vehicle conflict event identified by the proposed framework, illustrating the spatial proximity between the pedestrian and the approaching vehicle along with the associated surrogate safety indicators. The overlaid metrics, including Time-to-Collision (TTC), Post-Encroachment Time (PET), Time Exposed to TTC (TET), Time Integrated TTC (TIT), and braking-related parameters, are computed from trajectory-based estimations derived from automated detection and tracking. These values represent estimated safety indicators rather than direct physical measurements and are intended to characterize relative conflict severity and temporal risk exposure. The consistency between the observed spatial interaction, braking response, and low TTC values supports the classification of this event as a high-severity conflict within the adopted analytical framework.

Figure 7. TET and TIT

Figure 8 presents a comprehensive analytical summary of pedestrian crossing behavior observed during the study period, extending the trajectory- and conflict-based findings discussed in the preceding section. While previous analyses focused on interaction risk and infrastructure misalignment, this figure provides a behavioral decomposition of pedestrian crossing characteristics in terms of duration, spatial distribution, temporal exposure, and movement direction.

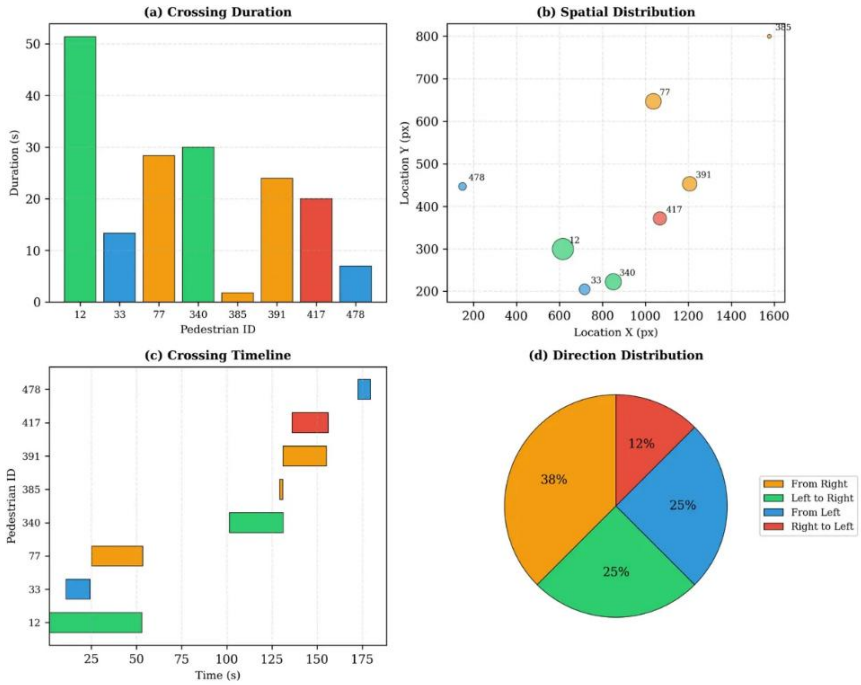

Figure 8. Conflicts Event

Figure 8 (a) shows substantial variability in crossing duration among individual pedestrians, with observed durations ranging from 2 to 51 seconds, indicating heterogeneous walking speeds and decision-making strategies under informal crossing conditions. Figure 8 (b) illustrates the spatial distribution of crossing events, revealing distinct clustering that identifies recurrent informal crossing hotspots, which represent critical locations for potential infrastructure intervention. The formation of these informal crossing clusters is not merely a violation of traffic rules but represents a rational behavioral response to minimize energy expenditure and travel time. This observation aligns with the findings of Retnowati et al. (2022) and Khalak et al. (2024), who argue that in developing urban contexts, pedestrian compliance is strongly negatively correlated with detour distance. The observed spatial discrepancy confirms that the current infrastructure fails

to capture the 'natural desire lines' connecting the school and the public park, forcing pedestrians to prioritize directness over formal safety measures.

Figure 8 (c) presents the temporal distribution of crossing events, highlighting differences in roadway exposure time. Longer occupancy durations are associated with increased interaction risk, while shorter, concentrated crossings reflect more decisive pedestrian behavior. Figure 8 (d) summarizes directional movement patterns, showing a dominant flow originating from one side of the corridor, alongside substantial bidirectional movement, underscoring the need for crossing facilities that accommodate asymmetric yet two-way pedestrian demand.

Table 1 also summarizes the descriptive statistics of the identified pedestrian–vehicle conflict events. The results indicate a mean Time-to-Collision (TTC) of 0.98 s (SD = 0.83), reflecting a high prevalence of critical interactions at the study location. Notably, 67% of the events with valid TTC values fall below the commonly adopted safety threshold of 1.5 s, underscoring the elevated risk level associated with these encounters. Post-Encroachment Time (PET) could be computed for only a limited subset of interactions (N = 2), suggesting that the majority of conflicts involved imminent collision scenarios rather than sequential path crossings with sufficient temporal separation. Vehicles engaged in conflict events exhibited a mean initial speed of 105.41 px/s and substantial evasive responses, as indicated by an average deceleration of 69.90 px/s². Additionally, the close spatial proximity between pedestrians and vehicles is evidenced by a mean minimum distance of 29.63 pixels (SD = 6.12), further highlighting the severity of the observed interactions.

The prevalence of critical TTC values (<1.5s) in this study (67%) indicates a conflict severity significantly higher than typical unsignalized intersections reported in similar mixed-traffic studies. This validates the effectiveness of the UAV-based surrogate safety assessment, echoing Singh et al. (2024) and Sun & Pei (2025), who demonstrated that trajectory-derived metrics provide a more sensitive indicator of latent risk than historical accident data alone. The low TTC values specifically reflect the aggressive interaction capability needed to navigate continuous traffic flows in the absence of spatial priority

Tabel 1. Summary Statistics of Surrogate Safety Measures

Variable	N	Mean	SD	Min	Max
Time to Collision (s)	24	0.98	0.83	0.02	2.74
Post Encroachment Time (s)	2	11.63	0.35	11.38	11.88
nitial Vehicle Speed (px/s)	21	105.41	96.07	1.02	319.90
Deceleration (px/s2)	21	69.90	109.59	-122.30	353.25
Braking Distance (px)	21	170.81	145.28	8.53	408.52
Minimum Distance (px)	31	29.63	6.12	1.18	47.27

CONCLUSION

Pedestrian crossing behavior is primarily driven by spatial accessibility rather than regulatory compliance. The observed misalignment between natural pedestrian desire lines and existing zebra crossing infrastructure generates systematic safety risks, evidenced by critical Time-to-Collision values and high-severity conflict exposure. The spatial concentration of informal crossings 135 meters from the designated facility reflects a structural design failure rather than a behavioral compliance issue. These findings validate automated trajectory analysis as a practical tool for evidence-based infrastructure planning in resource-constrained contexts. The integration of UAV-based detection with surrogate safety measures enables objective quantification of pedestrian-vehicle conflict risks without relying on labor-intensive manual observation. Future research should explore the temporal stability of desire line patterns across different time periods and evaluate post-intervention compliance rates following infrastructure relocation to validate the design-behavior alignment hypothesis in controlled settings.

ACKNOWLEDGEMENTS

The authors acknowledge the field survey team for their assistance during data collection.

REFERENCES

Ahmed, M. W., Adnan, M., Ahmed, M., Janssens, D., Wets, G., Ahmed, A., & Ectors, W. (2025). Drone-Enabled Behavioral Mapping of Pedestrian-Vehicle interactions on Zebra Crossings near Schools. *Transportation Research Procedia*, *91*, 131-138. https://doi.org/10.1016/j.trpro.2025.10.018

Al Bargi, W. A., Daniel, B. D., Khalifa, N. A., Rohani, M. M., Hussain, Q., & Hamdan, R. B. (2023). Modelling the utilization rates of pedestrian crosswalks. Heliyon, 9(9). https://doi.org/10.1016/j.heliyon.2023.e19310

Antwi, R. B., Lawson, P. L., Kimollo, M., Ozguven, E. E., Moses, R., Dulebenets, M. A., & Sando, T. (2025). Automated Detection of Pedestrian and Bicycle Lanes from High-Resolution Aerial Images by Integrating Image Processing and Artificial Intelligence (AI) Techniques. ISPRS International Journal of Geo-Information, 14(4). https://doi.org/10.3390/ijgi14040135

Ardiansah, A., Kadaryanto, B., & Oktapani, S. (2020). Kepatuhan Hukum Pejalan Kaki terhadap Penggunaan Sarana Penyeberangan di Kota Pekanbaru. Jurnal Wawasan Yuridika, 4(1), 47. https://doi.org/10.25072/jwy.v4i1.261

Bock, J., Krajewski, R., Moers, T., Runde, S., Vater, L., & Eckstein, L. (2019). The inD Dataset: A Drone Dataset of Naturalistic Road User Trajectories at German Intersections. http://arxiv.org/abs/1911.07602

Braun, M., Krebs, S., Flohr, F., & Gavrila, D. M. (2018). The EuroCity Persons Dataset: A Novel Benchmark for Object Detection. https://doi.org/10.1109/TPAMI.2019.2897684

Fourkiotis, M., Kazaklari, C., Kopsacheilis, A., & Politis, I. (2022). Applying deep learning techniques for the prediction of pedestrian behaviour on crossings with countdown signal timers. Transportation Research Procedia, 60, 536-543. https://doi.org/10.1016/j.trpro.2021.12.069

Ismail, A., Yusof, L. M., & Razlan, I. S. M. (2023). Pedestrian Behaviour at Unsignalized Zebra Crossing: A Case Study in UMP Gambang Campus. IOP Conference Series: Earth and Environmental Science, 1140(1). https://doi.org/10.1088/1755-1315/1140/1/012023

Jiang, J., Yan, K., Xia, X., & Yang, B. (2025). A Survey of Deep Learning-Based Pedestrian Trajectory Prediction: Challenges and Solutions. In Sensors (Vol. 25, Issue 3). Multidisciplinary Digital Publishing Institute (MDPI). https://doi.org/10.3390/s25030957

Khalak, A. A., Hussen, M., Ahmed, S., & Pandya, T. (2024). Pedestrian Safety at Signalized Intersections in Developing Countries: A Critical Appraisal. International Journal of Research Publication and Reviews Journal Homepage: Www.Ijrpr.Com, 5(2), 454-457. https://doi.org/https://doi.org/10.55248/gengpi.5.0224.0413

Li, N., Bai, X., Shen, X., Xin, P., Tian, J., Chai, T., & Wang, Z. (2024). Dense Pedestrian Detection Based on GR-YOLO. Sensors, 24(14). https://doi.org/10.3390/s24144747

Parra-Ovalle, D., Miralles-Guasch, C., & Marquet, O. (2023). Pedestrian street behavior mapping using unmanned aerial vehicles. A case study in Santiago de Chile. PLoS ONE, 18(3 March). https://doi.org/10.1371/journal.pone.0282024

Qin, G., Pan, R., Deng, Y., Mi, P., & Zhu, Y. (2025). Road pedestrian detection and tracking algorithm based on improved YOLOv5s and DeepSORT. PLOS ONE, 20(11 November). https://doi.org/10.1371/journal.pone.0334786

Redmon, J., & Farhadi, A. (2018). YOLOv3: An Incremental Improvement. https://arxiv.org/pdf/1804.02767

Retnowati, Fachrudin, H. T., & Mardianta, A. V. (2022). Walkability Study in Medan City Center Based on Pedestrian Perception: A Case Study off Merdeka And Kesawan Fields. International Journal of Education and Social Science Research, 05(05), 424-465. https://doi.org/10.37500/ijessr.2022.5524

Rosa, G. J. M., Afonso, J. M. S., Gaspar, P. D., Soares, V. N. G. J., & Caldeira, J. M. L. P. (2024). Detecting Wear and Tear in Pedestrian Crossings Using Computer Vision Techniques: Approaches, Challenges, and Opportunities. In Information (Switzerland) (Vol. 15, Issue 3). Multidisciplinary Digital Publishing Institute (MDPI). https://doi.org/10.3390/info15030169

Singh, D., Das, P., & Ghosh, I. (2024). Conflict-Based safety evaluations at unsignalized intersections using surrogate safety measures. Heliyon, 10(5). https://doi.org/10.1016/j.heliyon.2024.e27665

Sun, J., & Pei, Y. (2025). Behavior Spectrum-Based Pedestrian Risk Classification via YOLOv8-ByteTrack and CRITIC-Kmeans. Applied Sciences (Switzerland), 15(18). https://doi.org/10.3390/app151810008

Ünel, F. Ö., Özkalayci, B. O., & Çiğla, C. (2019). The Power of Tiling for Small Object Detection. 2019 IEEE/CVF Conference on Computer Vision and Pattern Recognition Workshops (CVPRW), 582-591. https://doi.org/10.1109/CVPRW.2019.00084

Zhang, Y., Sun, P., Jiang, Y., Yu, D., Weng, F., Yuan, Z., Luo, P., Liu, W., & Wang, X. (2022). ByteTrack: Multi-Object Tracking by Associating Every Detection Box. http://arxiv.org/abs/2110.06864